Archives available at journals.mriindia.com

International Journal of Advanced Electrical and Electronics Engineering

ISSN: 2278-8948

Volume 14 Issue 01, 2025

Design Of an Inductive Wireless Charging Station for Electric Vehicles with A Low-Power Experimental Validation of The Power-Transfer Chain

[1]Jinobin S U, [2]Renjith R, [3]Mahesh Kumar P, [4]Ezhil Vighnesh K

[1,2,3,4]Department of Electrical and Electronics Engineering, Stella Mary's College of Engineering, Aruthenganvilai, Kanyakumari District, Tamil Nadu, India

Peer Review Information

Submission: 09 March 2025
Revision: 11 April 2025
Acceptance: 05 May 2025

Keywords

Electric Vehicle, Wireless Power Transfer, Inductive Power Transfer, Resonant Coupling, SAE J2954, Qi Standard, Battery Management System, Foreign Object Detection, Charging Infrastructure.

Abstract

Conductive charging of electric vehicles (EVs) requires the user to handle a connector, exposes contacts to weather and mechanical wear, and presents a shock hazard in public installations. Wireless power transfer (WPT) removes the physical connector by coupling energy across an air gap between a ground-mounted transmitter coil and a vehicle-mounted receiver coil. This paper reports a two-part study. The first part is a design analysis of an inductive EV charging station: the conversion chain from AC mains through rectification, high-frequency inversion, resonant coupling, secondary rectification and battery management is specified; the governing resonance condition is stated; the applicable standards framework is reviewed, comprising SAE J2954, IEC 61980 and the Qi specification; and the safety provisions required for outdoor operation — electromagnetic shielding, foreign-object detection, thermal management and enclosure sealing — are defined. The second part is an experimental validation carried out at low power. A 12 W transformer, a four-diode full-wave rectifier and a 5 V inductive transmitter module were used to energise a receiver at a separation of approximately 2–5 cm. The receiver delivered 4.6–5 V with stable current across repeated trials, giving an estimated end-to-end efficiency of 70–75 % once transformer, rectification and coupling losses are accounted for; no component exceeded its safe operating temperature during testing. It is stated explicitly that this prototype operates roughly three orders of magnitude below EV charging power and therefore validates the principle of the conversion chain rather than the EV-scale design. A tariff and cost analysis for the Tamil Nadu context is included, and the measurements required to progress from the present demonstrator towards a deployable station are set out.

Introduction

Electric vehicles (EVs) have emerged as a practical alternative to internal-combustion vehicles, offering lower emissions, improved energy efficiency and reduced dependence on fossil fuels. Their adoption, however, is governed less by the vehicles than by the charging infrastructure available to support them. Charging stations address range anxiety — the concern that a vehicle will exhaust its charge before reaching the next charging point — and their distribution determines whether electric mobility is available equitably across urban, semi-urban and rural areas.

Conductive charging, in which the user connects a cable to the vehicle, is the established method but carries three recurring drawbacks: connectors wear with repeated use, exposed terminals present a safety risk in unsupervised public locations, and the operation is inconvenient in poor weather. Wireless power transfer (WPT) addresses all three by transferring energy across an air gap, eliminating the physical connector altogether.

This paper reports the design of an inductive wireless charging station for EVs together with an experimental validation of the conversion chain carried out at low power. The distinction between the two is maintained throughout: the design analysis addresses the EV-scale system, while the measurements of Section VI characterise a bench demonstrator operating far below EV power levels.

Figure 1: Electric vehicle charging infrastructure context.

1. Objectives

- To specify the conversion chain of an inductive EV charging station from mains input to vehicle battery.
- To review the standards and regulatory framework governing wireless EV charging.
- To define the safety provisions required for unattended outdoor operation.
- To validate the power-transfer chain experimentally and report the measured output and estimated efficiency.
- To analyse the charging cost and tariff structure applicable in the Tamil Nadu context.

Related Work

1. Evolution of EV Charging

Charging infrastructure has progressed from basic Level 1 AC charging to high-speed DC fast charging. These methods serve their purpose, but connector wear, safety risk from exposed terminals and the effort demanded of the user have sustained interest in contactless alternatives. Wireless charging addresses these limitations by enabling automatic and safe energy transfer without connectors.

2. Fundamentals of Wireless Power Transfer

WPT for EVs rests on magnetic resonance coupling or inductive coupling, in which power is transmitted through a magnetic field established between two coils: a transmitter embedded in the ground and a receiver mounted on the vehicle underside. Efficiency, coupling coefficient, coil alignment and coil design together determine the performance achieved.

3. Classification of Wireless Charging Systems

- Static wireless charging, in which transfer occurs while the vehicle is stationary, typically in a parking bay or garage.
- Dynamic wireless charging, in which transfer occurs while the vehicle is in motion, requiring coils embedded along the roadway.
- Stationary intermittent charging, a hybrid arrangement in which the vehicle pauses briefly at points along its route for a rapid energy top-up.

4. Key Components and Recent Advances

The major elements common to these arrangements are the primary and secondary coils that establish magnetic coupling; the power-electronics circuitry that converts and regulates power; the alignment system that ensures correct positioning; and the communication modules that exchange data between vehicle and charger. Recent work has introduced multi-coil systems, high-frequency inverters and alignment systems that improve both efficiency and positioning tolerance. Reported advances include inverters exceeding 90 % efficiency, bidirectional power flow supporting vehicle-to-grid operation, and modular coil arrays that widen the tolerance to misalignment [1], [3], [4].

5. Outstanding Challenges

- Sensitivity to misalignment between transmitter and receiver coils.
- Electromagnetic interference with nearby electronic equipment.
- System cost and complexity relative to conductive charging.

6. Standardisation and Regulatory Framework

Standardisation enables interoperability, so that a vehicle can charge safely at any compatible station irrespective of manufacturer or region, and it underpins consumer confidence and cost reduction. Three frameworks are relevant.

SAE J2954, developed by the Society of Automotive Engineers, is the leading standard for wireless power transfer in light-duty electric vehicles. It defines power levels up to 11 kW, alignment tolerance, communication between vehicle and charger, and safety measures.

IEC 61980, from the International Electrotechnical Commission, addresses electromagnetic compatibility, coil design and test procedures for WPT systems. The IEEE contributes further to global standards covering compatibility, efficiency and communication protocols.

The Qi specification, maintained by the Wireless Power Consortium, governs inductive charging over short distances and is the standard applied to the low-power demonstrator of Section VI. Qi operates over 110–205 kHz, typically achieves 70–85 % transfer efficiency, and mandates foreign-object detection, overvoltage protection, overcurrent protection and temperature control. Successive revisions extended the supported power from 5 W in Qi 1.0 to 15 W in Qi 1.2.3 and 1.2.4, while Qi2, released in 2023, introduces a magnetic power profile that improves alignment, reduces energy loss and enhances thermal management while retaining backward compatibility. Regulatory attention focuses in parallel on electromagnetic field exposure and interference, to protect public health and prevent disruption of nearby electronic devices.

System Architecture and Working Principle

The station is based on inductive power transfer and comprises two physically separated units. The transmitter unit is installed on or beneath the ground surface and connected to the AC supply. The receiver unit is mounted on the underside of the vehicle. When the vehicle is parked over the transmitter pad, power is transferred through the magnetic field established between the two coils, with power-electronic circuits converting, regulating and managing the flow. The conversion chain is shown in Fig. 2 and comprises nine stages: AC mains input; AC–DC conversion; high-frequency inversion; the primary transmitter coil; the air gap acting as coupling medium; the secondary receiver coil; rectification and filtering; the battery management system; and the battery pack as load.

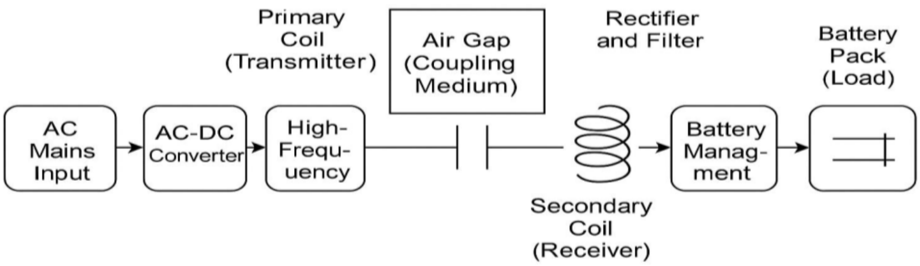

Figure 2: Block diagram of the wireless charging system, from AC mains input through resonant coupling to the vehicle battery pack.

In operation, the AC supply is first rectified to DC. This DC feeds a high-frequency inverter that drives the primary coil to generate an alternating magnetic field. When the receiver coil comes into proximity, the field induces a current in it; this current is rectified and filtered to charge the battery pack. The system operates at a resonant frequency — typically 85 kHz under SAE J2954 — chosen to maximise power transfer and efficiency.

1. Resonance Condition

Coil design governs the efficiency achieved. The two governing parameters are the coil inductance L and the capacitance C selected for resonance tuning, related by

$$f = 1 / (2\pi \sqrt{(LC)}) \quad (1)$$

A third parameter, the coupling coefficient k, depends on coil alignment and separation and determines what fraction of the generated flux links the receiver. Field strength, power loss and coupling efficiency may be verified in simulation using tools such as MATLAB/Simulink or ANSYS Maxwell before committing to a physical coil design.

2. Components of the Conversion Chain

- Microcontroller, for control and monitoring of the transfer process.
- MOSFETs or IGBTs, providing efficient switching in the inverter stage.
- Ferrite-core coils, forming the primary and secondary windings.
- Capacitors, selected for resonance tuning according to (1).
- Wireless communication module, for data exchange and alignment feedback.
- Display, for system status indication.
- Battery pack, as the storage element and load.

3. Coil Design

The transmitter coil is embedded in the charging pad and generates the alternating magnetic field. It is backed by a ferrite core that directs and concentrates flux upward, reducing stray loss. The winding is a flat spiral, or planar coil, wound in litz wire to limit skin and proximity effects at the operating frequency; turn counts typically range from 10 to 20 depending on the desired output power and frequency, and the inductance is chosen for efficient operation over 110–205 kHz. The receiver coil uses a comparable copper litz winding, is also ferrite-backed to maximise flux capture and minimise interference, and is dimensioned to match the transmitter for maximum coupling. Alignment between the two remains the dominant practical constraint on transfer efficiency. Figs. 3 to 5 show the coil arrangement, its integration with the battery and the resulting field geometry.

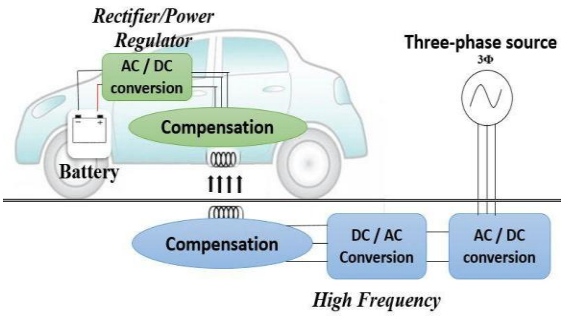

Figure 3: Charging coil arrangement.

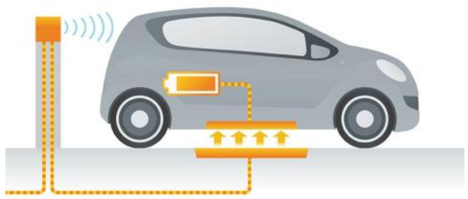

Figure 4: Integration of the receiver coil with the vehicle battery system.

Figure 5: Field coupling between the ground-based transmitter coil and the vehicle-mounted receiver coil, shown in side cutaway.

Fig. 5 illustrates the principle at vehicle scale: the field generated by the ground-based transmitter coil transfers power to the receiver installed within the vehicle undercarriage, eliminating the physical cable and requiring precise coil alignment for efficient transfer.

Design Specification and Safety Provisions

Table 1 gives the specification of the low-power charging arrangement adopted for the experimental work, which follows the Qi framework described in Section II-F.

Table 1. Parameter Specification of the Charging Arrangement

Parameter	Specification
Input voltage	5 V / 9 V (USB-C PD)
Output power	5 W / 10 W / 15 W
Efficiency	approximately 70–80 %
Operating frequency	110–205 kHz (Qi)
Safety features	OVP, OCP, OTP, FOD
Charging standard	Qi v1.2.4 or newer

1. Construction

At EV scale the transmitter pad is embedded in a non-conductive surface such as concrete or resin, sealed against water ingress and protected from mechanical stress. Alignment aids — magnetic markers or vision-based guides — assist the driver in positioning the vehicle correctly, and shielding is incorporated to limit electromagnetic interference and exposure to high-frequency fields.

The low-power demonstrator was constructed as a circular pad 90 mm in diameter and 12 mm high, with a tempered glass top, a silicone anti-slip ring, an ABS or anodised aluminium body and a ventilated rubberised base. A USB-C input at the rear accepts 5 V, 9 V or 12 V, and a multicolour LED ring indicates standby, charging and error states including foreign-object detection and overheating. Internally, input voltage is regulated by a buck or boost converter feeding a power-management stage that drives the transmitter coil, with a microcontroller managing the Qi protocol, foreign-object detection, LED indication and temperature monitoring through an NTC thermistor. Representative components include a wireless-charging transmitter IC, low on-resistance MOSFETs and a Qi-compliant transmitting coil. The arrangement supports a transfer distance of up to 8 mm at 75–85 % efficiency across the 5 W, 7.5 W, 10 W and 15 W power levels.

2. Safety Provisions

- Electromagnetic field shielding, to limit exposure to radiated fields.
- Foreign-object detection, inhibiting transfer when metallic objects are present in the gap.
- Thermal protection through temperature sensing, with heatsinks or forced air as required.
- Short-circuit and overvoltage protection on both primary and secondary sides.
- Insulated and sealed components rated for outdoor exposure.
- Compliance with ISO 15118 and SAE J2954 for wireless EV charging.

3. Advantages and Limitations

The arrangement offers three clear advantages: no physical connector, and therefore no connector wear; improved safety in public and domestic use; and compatibility with autonomous vehicle operation, where no driver is available to handle a cable. Three limitations are equally clear: higher cost than conductive charging; reduced efficiency under coil misalignment; and continuing immaturity for high-power fast-charging applications.

Battery Pack and Management Subsystem

1. Cell Configuration

The battery pack consists of multiple cells organised into modules within a protective casing. Cells are typically lithium-ion, connected in series and parallel to reach the required voltage and capacity. A battery management system (BMS) monitors temperature, voltage and current, and cooling by air or liquid manages the heat generated during charge and discharge. The assembly is mounted securely within the vehicle chassis, contributing structural support and crash protection. The pack used in the experimental work is shown in Fig. 6.

Figure 6: Battery pack assembly.

2. Cell Chemistry

Lithium-ion is the dominant chemistry, offering high energy density, long service life and low mass. Lithium iron phosphate is used where thermal stability and safety are prioritised, as in budget and commercial vehicles. Nickel-metal hydride, common in earlier hybrids, is now less used owing to its lower efficiency relative to lithium chemistries. A lithium-ion cell comprises a positive cathode and a negative anode separated by an electrolyte; lithium ions migrate from anode to cathode during discharge, releasing energy, and the process reverses during charge. Nominal cell voltage is approximately 3.6–3.7 V, higher than nickel-metal hydride or nickel-cadmium alternatives.

Reported advantages

- Energy density between 150 and 250 Wh/kg, suiting applications that require compact, lightweight storage.
- Cycle life extending to hundreds or thousands of charge–discharge cycles while retaining a substantial fraction of original capacity.
- Self-discharge of approximately 1–2 % per month, favourable for long standby periods.
- No memory effect, so partial discharge does not reduce usable capacity.
- Reported limitations
- Susceptibility to thermal runaway if damaged or improperly managed, with attendant fire risk.
- Performance and service life degraded by exposure to very high or very low temperatures.
- Environmental impact from extraction of lithium, cobalt and nickel, including water consumption in arid regions and documented ethical concerns in cobalt mining.
- Capacity degradation typically becoming significant after 500–1000 cycles.

3. Battery Management System

The BMS is central to safe operation. It balances charge across individual cells to prevent overcharge and deep discharge, protects against overcurrent, overvoltage, undervoltage and overheating, and governs the charge and discharge process so as to extend service life. Charging is terminated when cells reach their maximum voltage, typically 4.2 V per cell, and discharge is inhibited below approximately 3.0 V per cell.

State of charge and state of health

State of charge indicates the remaining charge and is tracked continuously from voltage measurement and current-flow analysis, accounting for cell age, temperature and usage pattern so that an accurate figure is available even where terminal voltage alone would be misleading. State of health describes the overall condition of the pack relative to its initial state, and is assessed from internal resistance, cycle count and capacity degradation; where it falls below a defined threshold, the system may alert the user or inhibit high-stress operations such as fast charging.

Cell balancing

Cells within a series string diverge in voltage and capacity through manufacturing variance and operational history. Balancing equalises charge across the string so that each cell operates within its optimal range, maximising usable pack capacity and preventing individual cells from being overcharged or over-discharged. Three approaches are used. Passive balancing dissipates excess charge from higher-voltage cells through resistors; it is simple and inexpensive but wastes energy and is less effective where voltage differences are large. Active balancing transfers charge between cells using switching circuitry and control algorithms, achieving higher efficiency and better accuracy. Hybrid balancing applies passive balancing as the primary method and active balancing where greater precision is required, trading cost against accuracy.

4. Charging Requirements

Charging a four-cell lithium series pack of nominal 20 V and 2 Ah capacity requires a lithium-compatible charger delivering a slightly higher voltage, typically 21 V to 21.5 V, to reach full charge without overvoltage. A constant-current, constant-voltage (CC-CV) profile is standard for lithium chemistries. A charging current of 1 A to 2 A is appropriate for a 2 Ah pack, avoiding overheating and cell damage. The charger should provide a maximum of 4.2 V per cell, and should terminate charging when the current falls to approximately 10 % of its initial value. Overcharge, short-circuit, temperature and reverse-polarity protections are required, and a BMS must be fitted to balance the cells and safeguard the pack.

Figure 7: Wireless charging station arrangement.

Experimental Results

The experimental system was assembled from a 12 W AC transformer providing voltage step-down, a full-wave rectifier of four diodes converting AC to DC, and a 5 V wireless transmitter module driving a receiver module positioned at a separation of approximately 2 to 5 cm.

1. Measured Output

The receiver delivered an output measured at approximately 4.6 V to 5 V, with a stable current suitable for charging small electronic devices such as a smartphone or a microcontroller-based battery. Power transfer was reliable at close range with minimal misalignment, and the system performed consistently across repeated trials.

Table 2. Measured Performance of the Experimental Power-Transfer Chain

Quantity	Value	Status
Transformer rating	12 W	specified
Rectifier	Four-diode full-wave	specified
Transmitter module supply	5 V	specified
Coil separation	approximately 2–5 cm	measured
Receiver output voltage	4.6–5 V	measured
Estimated end-to-end efficiency	70–75 %	estimated
Component temperature rise	No significant overheating	observed

2. Efficiency and Thermal Behaviour

End-to-end efficiency was estimated at approximately 70–75 %, accounting for losses in the transformer, in diode rectification and in the inductive coupling itself. This figure is an estimate derived from the measured input and output rather than a calorimetric determination, and is reported as such in Table II. No significant overheating was observed during testing and all components remained within safe operating temperatures.

3. Battery and Charging-Time Calculation

The storage element used in the experimental arrangement was specified as follows: battery voltage 5 V; battery capacity 2.2 Ah; input current 3 A; solar contribution 1 A; total available charging current 4 A. On this basis the charging time is

Charging time = Battery capacity / Input current (2)

which for the stated values gives 2.2 Ah / 2 A = 0.55 h, or approximately 33 minutes. It should be noted that the source record states both a 2 A and a 4 A available current at different points; the calculation above uses the 2 A figure, from which the quoted charging time follows.

4. Solar Contribution

A solar panel supplements the supply to the charging arrangement. Panel orientation was examined during the trials, and a tilt of 45° was adopted as the fixed-mount compromise. This angle favours absorption during winter months when the sun is lower, at some cost to summer performance, and yields a more consistent year-round output than a shallower fixed tilt in temperate latitudes. Output was observed to depend on available light, with reduced yield at peak midday heat. For maximum performance the tilt should be computed from the latitude of the installation and the seasonal demand profile rather than fixed at a nominal value.

Figure 8: Solar panel providing supplementary supply to the charging arrangement.

5. Scope of the Validation

The scope of this result must be stated precisely. The demonstrator transfers approximately 5 W across a 2–5 cm gap, whereas an EV charging station under SAE J2954 operates up to 11 kW across a gap of the order of 15–25 cm. The prototype is therefore roughly three orders of magnitude below EV charging power. It validates the operating principle of the conversion chain — rectification, inversion, inductive coupling, secondary rectification — and confirms that the chain delivers a stable regulated output at the efficiency expected of a Qi-class link. It does not validate the EV-scale design of Sections III and IV, and no claim to that effect is made here.

Cost and Tariff Analysis

At the time of the study no public wireless EV charging station was available in Nagercoil or elsewhere in Tamil Nadu, and wireless charging remained at an early stage of deployment in India. The state's programme of subsidies for EV charging infrastructure may in future extend to wireless installations. The tariff structure applicable to public EV charging stations in Tamil Nadu, as set by the Tamil Nadu Electricity Regulatory Commission, is given in Table 3.

Table 3. TNERC Time-of-Day Tariff for Public EV Charging Stations

Period	Tariff (₹ per unit)
10:00–14:00 and 23:00–05:00	8
05:00–10:00 and 14:00–18:00	10
18:00–23:00	12

Charging-station cost comprises energy charges per kWh consumed; fixed charges per kW per month based on maximum demand; time-of-day charges that vary by period so as to encourage off-peak use; and service charges for additional facilities such as battery swapping or fast charging. Time-of-day structures generally distinguish solar hours, from approximately 09:00 to 16:00, when rates are lower because solar generation is abundant, from non-solar hours when demand is higher and conventional generation dominates. Draft national guidelines have proposed ₹3.00/kWh for AC charging during solar hours and ₹4.00/kWh outside them, and ₹11.00/kWh and ₹13.00/kWh respectively for DC fast charging; these are subject to revision by state regulation.

Goods and services tax on wireless charging stations was recorded as 18 % across the states surveyed, namely Andhra Pradesh, Chhattisgarh, Goa, Gujarat, Haryana, Sikkim and Tamil Nadu.

Discussion

Two findings emerge from the work. The first is that the inductive conversion chain behaves as predicted at low power: the measured 4.6–5 V output at 70–75 % estimated efficiency falls within the 70–85 % band that the Qi specification anticipates for a short-gap link, which supports the design analysis of Section III at the level of principle.

The second is the size of the gap between that demonstrator and a deployable EV station. The gap is not merely one of scale. Increasing transfer power by three orders of magnitude changes the dominant engineering problems: thermal management ceases to be a matter of confirming that nothing gets hot and becomes a design driver; electromagnetic exposure moves from negligible to regulated; foreign-object detection becomes a safety-critical function rather than a convenience; and the 15–25 cm ground clearance of a vehicle reduces the coupling coefficient far below that achieved across the 2–5 cm gap measured here. Each of these is addressed in the design analysis and none is exercised by the experiment.

The measurements required to close the gap are therefore specific: transfer efficiency measured as a function of coil separation across the vehicle-relevant range; efficiency measured as a function of lateral misalignment; thermal rise under sustained operation at rated power; and field-strength measurement against the exposure limits set by the applicable standard. Until those are available, the EV-scale design remains an analysis rather than a validated result.

Limitations

- The experimental validation operates at approximately 5 W across a 2–5 cm gap and does not test the EV-scale design; the two are reported separately throughout.
- Efficiency is estimated from measured input and output rather than determined calorimetrically, and is quoted as a range.
- Neither misalignment tolerance nor efficiency against separation was characterised; both are central to EV-scale performance.
- No electromagnetic field measurement was made, so compliance with exposure limits is not demonstrated.
- Foreign-object detection and thermal protection are specified in the design but were not exercised under fault conditions.
- The tariff analysis reflects rates current at the time of study and is subject to regulatory revision.

Conclusion

A design analysis and a low-power experimental validation of an inductive wireless charging station for electric vehicles have been presented. The design specifies the conversion chain from AC mains through rectification, high-frequency inversion, resonant coupling at approximately 85 kHz, secondary rectification and battery management; states the resonance condition governing coil and capacitor selection; reviews the SAE J2954, IEC 61980 and Qi standards framework; and defines the shielding, foreign-object detection, thermal and sealing provisions required for outdoor operation.

Experimentally, a 12 W transformer, a four-diode full-wave rectifier and a 5 V transmitter module delivered 4.6–5 V at the receiver across a 2–5 cm gap, at an estimated end-to-end efficiency of 70–75 %, with no component exceeding its safe operating temperature and consistent behaviour across repeated trials. This result validates the principle of the conversion chain; it does not validate the EV-scale design, from which it is separated by roughly three orders of magnitude in transfer power, and the paper states this distinction rather than eliding it.

The contribution is a specified design together with an honest account of what has and has not been demonstrated, and a defined set of measurements — efficiency against separation and misalignment, thermal rise at rated power, and field-strength compliance — by which the design could be carried towards deployment.

Future Scope

Table 4 sets out the power levels, charging durations and use cases anticipated for wireless charging across vehicle classes. These are projected deployment scenarios drawn from the wider literature, not measurements from this work.

Table 4. Projected Wireless Charging Scenarios by Power Level

Charging power	Full charge time	Vehicle type	Use case	Utilisation potential
3.3 kW (low)	8–12 h	Compact EVs	Home, overnight charging	Low to moderate
7.7 kW (medium)	4–8 h	Sedans, small SUVs	Public parking, workplaces	Moderate
11 kW (high)	3–6 h	Larger EVs, delivery vans	Fleet depots, garages	Moderate to high
22 kW (fast wireless)	1.5–3 h	Taxis, commercial fleets	Taxi ranks, high-turnover parking	High
50–100 kW (dynamic)	Ongoing while driving	Public transit, trucks	Inductive roads, in-motion charging	Very high

A financial projection for a single station over its first four operating years was prepared on the basis of rising capacity utilisation, and is reproduced in Table 5. These figures are projections dependent on assumed utilisation and tariff, not observed revenues, and should be treated accordingly.

Table 5. Projected Station Economics by Operating Year

Year	CUF	Daily energy (kWh)	Annual revenue (₹)	Annual operating expense (₹)	Net (₹)
1	15 %	150	5,47,500	2,90,000	2,57,500
2	25 %	250	9,12,500	3,00,000	6,12,500
3	40 %	400	14,60,000	3,10,000	11,50,000
4	65 %	650	23,72,500	3,20,000	20,52,500

Beyond these projections, the priorities identified for further work are the characterisation measurements listed in Section VIII; integration of bidirectional operation to support vehicle-to-grid energy flow; extension of the alignment system to reduce sensitivity to parking accuracy; and progression from static charging towards the dynamic in-motion case, which depends on both roadway coil installation and the regulatory framework for embedded infrastructure.

Acknowledgment
The authors thank the Department of Electrical and Electronics Engineering, Stella Mary's College of Engineering, for laboratory facilities and guidance throughout the project.

References

M. Yilmaz and O. Keysan, "Review of charging technologies for electric vehicles," IEEE Transactions on Industrial Electronics, vol. 61, no. 5, May 2014.

M. A. Mohamed et al., "Design and implementation of a Qi-compliant wireless power transfer system," in Proc. 2018 IEEE Wireless Power Transfer Conference (WPTC), 2018.

S. Lukic and Z. Pantic, "Cutting the cord: static and dynamic inductive wireless charging of electric vehicles," IEEE Electrification Magazine, vol. 1, no. 1, 2013.

Z. Zhang, W. Li, C. C. Mi and Y. Zhang, "Design and implementation of a primary-side controlled wireless charging system for electric vehicles," IEEE Journal of Emerging and Selected Topics in Power Electronics, vol. 3, no. 1, Mar. 2015.

K. H. Kim, D. H. Kim, J. Kim, S. Y. Choi and C. T. Rim, "Design of a wireless power transfer system with multiple self-regulated and cooperatively regulated secondary coils," IEEE Transactions on Power Electronics, vol. 30, no. 11, Nov. 2015.

C. T. Rim and C. Mi, Wireless Power Transfer for Electric Vehicles and Mobile Devices. IEEE Press, 2017.

S. Li and C. C. Mi, "Wireless power transfer for electric vehicle applications," IEEE Journal of Emerging and Selected Topics in Power Electronics, vol. 3, no. 1, Mar. 2015.

J.-M. Kim et al., "Analysis of a resonant coil for wireless power transfer with high efficiency," IEEE Transactions on Industrial Electronics, 2014.

A. P. Sample, D. A. Meyer and J. R. Smith, "Analysis, experimental results, and range adaptation of magnetically coupled resonators for wireless power transfer," IEEE Transactions on Industrial Electronics, 2011.

M. Amjad, M. Farooq-i-Azam, Q. Ni, M. Dong and E. A. Ansari, Renewable and Sustainable Energy Reviews, vol. 167, 2022.

S. H. Yusoff, A. A. Abdullah, N. N. Nanda and A. S. A. Badawi, IIUM Engineering Journal, vol. 23, no. 1, 2022.

K. Divya, K. E. Vignesh, Ch. Narendra Kumar, and T. Rajesh, "Comparison of PI and AI Controllers Used for DC-DC Converter for EV Fast Charging," Journal of Critical Reviews, vol. 7, no. 6, pp. 1290–1298, 2020, doi: 10.31838/jcr.07.06.226.